HHS Public Access

Author manuscript

Small. Author manuscript; available in PMC 2021 April 01.

Published in final edited form as:

Small. 2020 April ; 16(16): e1905910. doi:10.1002/smll.201905910.

Gelatin methacryloyl microneedle patches for minimally-invasive extraction of skin interstitial fluid

Jixiang Zhu,
Department of Bioengineering, Henry Samueli School of Engineering and Applied Sciences, University of California, Los Angeles, Los Angeles, CA 90095, USA

Center for Minimally Invasive Therapeutics (C-MIT), University of California, Los Angeles, Los Angeles, CA 90095, USA

Department of Biomedical Engineering, School of Basic Medical Sciences, Guangzhou Medical University, Guangzhou 511436, China

Affiliated Stomatology Hospital of Guangzhou Medical University, Guangzhou 511436, China

Xingwu Zhou,
Department of Bioengineering, Henry Samueli School of Engineering and Applied Sciences, University of California, Los Angeles, Los Angeles, CA 90095, USA

Center for Minimally Invasive Therapeutics (C-MIT), University of California, Los Angeles, Los Angeles, CA 90095, USA

Han-Jun Kim,
Department of Bioengineering, Henry Samueli School of Engineering and Applied Sciences, University of California, Los Angeles, Los Angeles, CA 90095, USA

Center for Minimally Invasive Therapeutics (C-MIT), University of California, Los Angeles, Los Angeles, CA 90095, USA

Moyuan Qu,
Department of Bioengineering, Henry Samueli School of Engineering and Applied Sciences, University of California, Los Angeles, Los Angeles, CA 90095, USA

Center for Minimally Invasive Therapeutics (C-MIT), University of California, Los Angeles, Los Angeles, CA 90095, USA

Xing Jiang,
Department of Bioengineering, Henry Samueli School of Engineering and Applied Sciences, University of California, Los Angeles, Los Angeles, CA 90095, USA

Center for Minimally Invasive Therapeutics (C-MIT), University of California, Los Angeles, Los Angeles, CA 90095, USA

School of Nursing, Nanjing University of Chinese Medicine, Nanjing 210023, China

[*] khademh@ucla.edu, sunwj@ucla.edu.

Supporting Information

Supporting Information is available from the Wiley Online Library or from the author.

KangJu Lee,
Department of Bioengineering, Henry Samueli School of Engineering and Applied Sciences, University of California, Los Angeles, Los Angeles, CA 90095, USA

Center for Minimally Invasive Therapeutics (C-MIT), University of California, Los Angeles, Los Angeles, CA 90095, USA

Li Ren,
Department of Bioengineering, Henry Samueli School of Engineering and Applied Sciences, University of California, Los Angeles, Los Angeles, CA 90095, USA

Center for Minimally Invasive Therapeutics (C-MIT), University of California, Los Angeles, Los Angeles, CA 90095, USA

Qingzhi Wu,
Department of Bioengineering, Henry Samueli School of Engineering and Applied Sciences, University of California, Los Angeles, Los Angeles, CA 90095, USA

Center for Minimally Invasive Therapeutics (C-MIT), University of California, Los Angeles, Los Angeles, CA 90095, USA

Canran Wang,
Department of Bioengineering, Henry Samueli School of Engineering and Applied Sciences, University of California, Los Angeles, Los Angeles, CA 90095, USA

Center for Minimally Invasive Therapeutics (C-MIT), University of California, Los Angeles, Los Angeles, CA 90095, USA

Xunmin Zhu,
Department of Biomedical Engineering, School of Basic Medical Sciences, Guangzhou Medical University, Guangzhou 511436, China

Affiliated Stomatology Hospital of Guangzhou Medical University, Guangzhou 511436, China

Peyton Tebon,
Department of Bioengineering, Henry Samueli School of Engineering and Applied Sciences, University of California, Los Angeles, Los Angeles, CA 90095, USA

Center for Minimally Invasive Therapeutics (C-MIT), University of California, Los Angeles, Los Angeles, CA 90095, USA

Shiming Zhang,
Department of Bioengineering, Henry Samueli School of Engineering and Applied Sciences, University of California, Los Angeles, Los Angeles, CA 90095, USA

Center for Minimally Invasive Therapeutics (C-MIT), University of California, Los Angeles, Los Angeles, CA 90095, USA

Junmin Lee,
Department of Bioengineering, Henry Samueli School of Engineering and Applied Sciences, University of California, Los Angeles, Los Angeles, CA 90095, USA

Center for Minimally Invasive Therapeutics (C-MIT), University of California, Los Angeles, Los Angeles, CA 90095, USA

Nureddin Ashammakhi,
Department of Bioengineering, Henry Samueli School of Engineering and Applied Sciences, University of California, Los Angeles, Los Angeles, CA 90095, USA

Center for Minimally Invasive Therapeutics (C-MIT), University of California, Los Angeles, Los Angeles, CA 90095, USA

Samad Ahadian,
Department of Bioengineering, Henry Samueli School of Engineering and Applied Sciences, University of California, Los Angeles, Los Angeles, CA 90095, USA

Center for Minimally Invasive Therapeutics (C-MIT), University of California, Los Angeles, Los Angeles, CA 90095, USA

Mehmet Remzi Dokmeci,
Department of Bioengineering, Henry Samueli School of Engineering and Applied Sciences, University of California, Los Angeles, Los Angeles, CA 90095, USA

Center for Minimally Invasive Therapeutics (C-MIT), University of California, Los Angeles, Los Angeles, CA 90095, USA

Department of Radiology, David Geffen School of Medicine, University of California, Los Angeles, Los Angeles, CA 90095, USA

Zhen Gu,
Department of Bioengineering, Henry Samueli School of Engineering and Applied Sciences, University of California, Los Angeles, Los Angeles, CA 90095, USA

Center for Minimally Invasive Therapeutics (C-MIT), University of California, Los Angeles, Los Angeles, CA 90095, USA

Jonsson Comprehensive Cancer Center, University of California, Los Angeles, Los Angeles, CA90095, USA

California NanoSystems Institute, University of California, Los Angeles, Los Angeles, CA90095, USA

Wujin Sun[*],
Department of Bioengineering, Henry Samueli School of Engineering and Applied Sciences, University of California, Los Angeles, Los Angeles, CA 90095, USA

Center for Minimally Invasive Therapeutics (C-MIT), University of California, Los Angeles, Los Angeles, CA 90095, USA

Ali Khademhosseini[*]
Department of Bioengineering, Henry Samueli School of Engineering and Applied Sciences, University of California, Los Angeles, Los Angeles, CA 90095, USA

Center for Minimally Invasive Therapeutics (C-MIT), University of California, Los Angeles, Los Angeles, CA 90095, USA

Jonsson Comprehensive Cancer Center, University of California, Los Angeles, Los Angeles, CA90095, USA

California NanoSystems Institute, University of California, Los Angeles, Los Angeles, CA90095, USA

Department of Radiology, David Geffen School of Medicine, University of California, Los Angeles, Los Angeles, CA 90095, USA

Department of Chemical and Biomolecular Engineering, Henry Samueli School of Engineering and Applied Sciences, University of California, Los Angeles, Los Angeles, CA 90095, USA

California NanoSystems Institute, University of California, Los Angeles, Los Angeles, CA90095, USA

Center of Nanotechnology, Department of Physics, King Abdulaziz University, Jeddah 21569, Saudi Arabia

Department of Bioindustrial Technologies, College of Animal Bioscience and Technology, Konkuk University, Seoul 143701, Republic of Korea

Abstract

The extraction of interstitial fluid (ISF) from skin using microneedles (MNs) has attracted growing interest in recent years due to its potential for minimally invasive diagnostics and biosensors. ISF collection by absorption into a hydrogel MN patch is a promising way that requires the materials to have outstanding swelling ability. Here, we have developed a gelatin methacryloyl (GelMA) patch with an 11 × 11 array of MNs for minimally invasive sampling of ISF. The properties of the patch can be tuned by altering the concentration of the GelMA prepolymer and the crosslinking time; patches are created with swelling ratios between 293% and 423% and compressive moduli between 3.34 MPa to 7.23 MPa. The optimized GelMA MN patch demonstrated efficient extraction of ISF. Furthermore, it efficiently and quantitatively detects glucose and vancomycin in ISF in an *in vivo* study. This minimally invasive approach of extracting ISF with a GelMA MN patch has the potential to complement blood sampling for the monitoring of target molecules from patients.

Abstract

A novel microneedle patch based on gelatin methacryloyl is developed for minimally invasive sampling of interstitial fluid (ISF). The properties of the patch can be tuned by altering the concentration of prepolymer and the crosslinking time. Furthermore, the MN approach efficiently detects glucose and vancomycin in ISF. This ISF extraction strategy has the potential to provide a support of target molecule detection in clinic.

Graphical Abstract

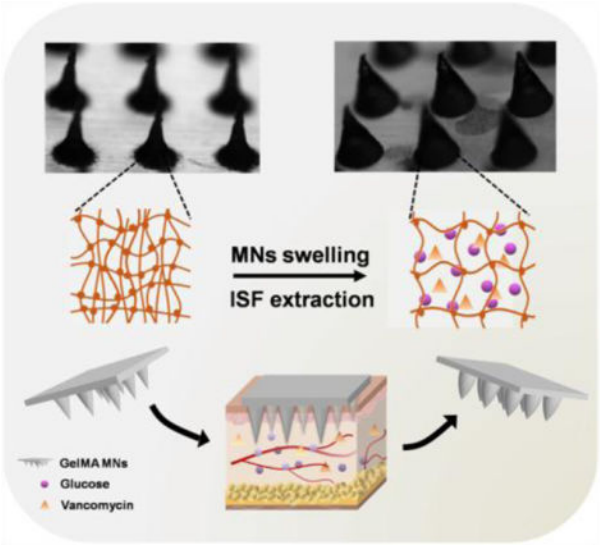

Keywords

microneedles; gelatin methacryloyl; skin interstitial fluid; transdermal extraction; minimally invasive

The ability to detect biomarkers and drugs with minimally invasive methods has attracted widespread attention due to its promise to revolutionize patient screening and the diagnosis of disease. Currently, blood sampling is the clinical standard for tracking patient health and disease progression.[1] However, obtaining blood is generally invasive and may be complicated by infection or anxiety. Moreover, veins that are mechanically weak and prone to collapse increase the difficulty of collecting blood. Beyond the challenges associated with blood collection, circulating blood also has its limit for providing healthcare-related information. In some cases, drug concentration in the blood is poorly correlated with concentration at the target site; some antibiotics have been shown to distribute differently in the blood compared to muscle or other tissues.[2] As a result, there is growing interest in developing alternatives to blood sampling that can provide accurate information about an individual's health status with minimal patient discomfort.

Body fluids other than blood have been investigated for biomarker detection or drug monitoring including interstitial fluid (ISF), saliva, and urine.[3] Saliva and urine sampling are less invasive, but they are limited by their low biomarker content and fluctuating volume.[4] ISF serves as an intermediate between cells and the circulatory system as it surrounds cells throughout the body and acts as a reservoir for biomolecules, nutrients, and waste.[5] Previous studies have demonstrated that protein concentration in ISF is conserved in relation to serum, and nearly all proteins present in serum can be detected in ISF.[6] Moreover, the protein content of ISF is lower than that of blood, facilitating the collection of drugs in their active form and simplifying the detection of some molecules.[7] Furthermore, some biomarkers in ISF are unique as they are not found in serum, suggesting that sampling ISF could expand beyond the diagnostic capabilities of serum for certain diseases.[8]

Sourcing ISF can be simpler than other body fluids. Skin is the largest organ of the human body and is the most convenient source of ISF. Skin ISF is rich in systemic metabolites, biomarkers, as well as drugs.[9] However, the outermost layer of the epidermis, the stratum corneum, is a natural barrier restricting the exchange of fluid. In previous studies, skin ISF has been sampled by a variety of techniques including suction blisters, which require elevated vacuum for > 1 h but may cause lasting skin damage;[6, 8] reverse iontophoresis, which is limited to small molecules and requires specialized equipment operated by a trained professional;[10] or microdialysis, which requires local anesthesia and medical training.[11, 12] All these collection procedures are time-consuming and limited by the prerequisite specialized equipment and medical expertise. Therefore, a simple and minimally invasive technique that is capable of extracting sufficient quantities of ISF from the skin is urgently needed.

One promising approach for ISF extraction is the use of microneedle (MN) array patches.[13–15] Historically, MNs were developed for the delivery of drugs,[16–18] vaccines,[19,20] biomolecules,[21, 22] or stem cells.[23] The extensive focus on developing MN-based delivery approaches rather than extraction methods may be the result of the lack of excellent ISF-absorbing materials. MNs typically have a length less than 1 mm with tips much sharper than hypodermic needles. Such geometric designs enable MNs to efficiently pierce the stratum corneum and form microscale ISF extraction channels without touching blood vessels, nerve fibers, or their endings present in the epidermis or dermis. Due to their small size and short depth of penetration, MNs provide a painless, simple, and minimally invasive way to sample skin ISF. To evaluate patient compliance with MN-based diagnostics, Mooney *et al.* interviewed 16 parents with experience of premature birth and the interviewees preferred MN-mediated monitoring over traditional blood sampling in neonates.[24] Based on MNs-mediated fluid extraction strategy, Chang *et al.* achieved offline analysis of metabolites such as glucose and cholesterol.[25] Zhang *et al.* devised encoded MNs capable of detecting multiple biomarkers (TNF-α, IL-1β, IL-6).[26] Sulaiman *et al.* developed MNs coated with an alginate-peptide nucleic acid hybrid material for specific nucleic acid sampling and detection.[27] Furthermore, the extraction of plant DNA by MNs was demonstrated for rapid detection of plant diseases.[28]

Previously, we have demonstrated that gelatin methacryloyl (GelMA) is a suitable material for the fabrication of MNs as it has good biocompatibility and desirable drug delivery properties.[29] The nature-derived GelMA MN patch possesses good biocompatibility as a medical device for sourcing ISF in a convenient and minimally invasive manner. The GelMA MN patch also has advantages in lower fabrication cost and higher production yield when comparing to other nature-derived material-based MN patches, such as those from hyaluronic acid, making it a competitive platform for translational studies. In this study, GelMA MN patches were prepared with various crosslinking degrees and initial polymer concentrations. By tuning these parameters, swelling and other mechanical properties of the MN were optimized for the rapid extraction of ISF.

The fabrication process of the GelMA MN patches is outlined in Figure 1A. The patch was prepared by a micro-molding approach, in which GelMA prepolymer was cast into a pre-designed mold by centrifugation. The microstructure of the individual MNs is presented in

Figure 1B–E (the initial GelMA concentration is 20 %). Both the top and side views show conical MN structure. Magnified images indicate that the height and bottom diameter of the single needle were about 600 and 300 μm, respectively. Figure 1F is the optical microscopic image of the GelMA MN patch, which showed an 11 ×11 array of uniformly aligned MNs fixed on a 1 cm ×1 cm patch to support sufficient ISF extraction for later analysis. The most commonly used techniques to manufacture MNs with different shapes and sizes include micromolding,[30] lithography,[31] laser cutting,[32] three-dimensional (3D) printing,[33] and wet or dry etching.[34] In the present work, we used a polydimethylsiloxane (PDMS) mold with a pre-designed shape and size to manufacture the MN patches. The prepared MNs are 600 μm in height, which is optimal for penetrating of the stratum corneum and preventing the skin wrapping effect.[35]

The swelling and mechanical properties of various GelMA MNs patches are shown in Figure 2. The dimensions of the patches changed and achieved equilibrium upon immersion in DPBS solution for 24 h. As shown in Figure 2A, final swelling ratios ranged from 293 ± 69% to 423 ± 62% as the initial GelMA concentration was varied from 25% to 10% (m/v) and the crosslinking time was set to 200 s. We observed that the swelling ratio is inversely correlated with the GelMA concentration. Figure 2B shows that the final swelling ratios varied between 337 ± 67% and 410 ± 79% as the crosslinking time was changed from 300 s to 10 s when initial GelMA concentration was 20% (m/v). Longer crosslinking exposures lead to lower swelling ratios of the GelMA MN patches in the first 10 min. Similar trend has also been observed at other concentrations of gelatin.[36–38] It is also worth noting that rapid swelling was observed in the first 10 min following immersion in DPBS solution, indicating rapid liquid absorption by the patches. Stress-strain curves of various GelMA patches with different initial concentrations and crosslinking time are presented in Figure 2C and 2D, respectively. Enhanced mechanical properties, such as increased compressive stress, were observed with elevated initial GelMA concentrations or increased crosslinking time. The compressive modulus was found to increase non-linearly from 3.35 ± 0.62 MPa to 7.21 ± 1.74 MPa when the GelMA concentration was increased from 10% (m/v) to 25% (m/v). Interestingly, the compressive modulus did not change significantly below a concentration of 20% (m/v), but nearly doubled to 5.80 MPa at 20% (m/v) (Figure 2E). Furthermore, it was observed that the compressive modulus changed from 3.34 ± 1.33 MPa to 7.23 ± 1.66 MPa when the crosslinking time was varied from 10 to 300 s (Figure 2F). Many polymeric MNs presented good mechanical strength. One example is MN made from polylacite (PLA). Li *et al.* studied the mechanical property of PLA MNs and the results showed a single PLA MN patch with the height of 600 μm maintained good skin penetration efficiency after 20 times of insertion.[39] However, the PLA MNs was not able to obtain ISF extraction because of the hydrophobic nature. Mandal *et al.* fabricated alginate coated PLA MNs to sample cells and fluid for monitoring skin resident immunity. The elastic modulus of alginate coating was about 1 kPa, which could bring sufficient mechanical stiffness for penetration.[40] Hyaluronic acid (HA)-based MNs have also presented good mechanical property when applied in ISF extraction and drug delivery. The mechanical property of HA MNs was tunable by changing the doses of loaded drug.[41] Furthermore, Lin *et al.* studied the mechanical property of HA/cyclodextrin composite MNs. By changing the material composition, they produced MNs of higher mechanical strength for successful insertion into

the compact and hard scar tissue[42]. Comparing to these MNs, our study demonstrated the mechanical strength of GelMA MNs was tunable in terms of the initial GelMA concentration and crosslinking time. We have also studied the influence of methacrylation degree on the swelling ratio and mechanical property of GelMA in our previous work.[43] The results indicated that a higher degree of methacrylation led to a lower swelling ratio or stronger mechanical property when the concentration of initial GelMA was constant. The methacrylation degree of GelMA was defined as the ratio of methacrylate groups to the total amino groups presented in gelatin prior to reaction. It can be estimated from the integrated intensities of peaks in ^{1}H NMR spectra (Figure S1),[44, 45] which was approximately 71% in the present work.

A series of MN designs have been reported corresponding to different ISF sampling mechanisms including (1) diffusion, (2) capillary action, (3) osmosis, and (4) pressure driven convection.[46] These mechanisms are affected by the shape, size, and material of MNs. Among the mechanisms of obtaining ISF from skin using MN patches, ISF collection by diffusion into a hydrogel has not been effective in comparison to the other collection mechanisms.[46] This is mainly due to material properties, especially swelling ratio, rather than a fundamental limitation of the approach. To overcome this challenge, a material with a high swelling ratio is desired for ISF extraction by diffusion. GelMA was selected due to its biocompatibility and composition of primarily gelatin,[47] a natural polymer already used in biomedical engineering applications in our previous studies, such as scaffolds,[48] injectable hydrogels,[49] drugs and growth factor carriers,[50] and bioinks for 3D printing.[51] We observed that the GelMA had swelling properties promising for the extraction of ISF. In the present work, we demonstrate that higher initial concentrations of GelMA lead to mechanically stronger GelMA MNs. Meanwhile, increasing GelMA concentration results in suppressed swelling ratios. A notable increase in compressive modulus has been found between GelMA concentrations of 25% (w/v) and 10% (w/v). Microstructures of MN patches fabricated with different initial GelMA concentrations (10%, 15%, 20% and 25%) were also examined by SEM (Figure S2). The MN patches with initial GelMA concentration of 10% showed obvious shrinkage while those with higher initial concentrations (15%, 20% and 25%) presented similar morphology and limited shrinkage. The shrinkage led to a change of MN morphology that might affect the mechanical properties of MN patch. We further tested the skin penetration of GelMA MN patches with different initial concentrations and the results showed that the patches can efficiently penetrate the skin when the initial GelMA concentrations were ≥ 20% (w/v) (Figure S3). Considering the swelling property, GelMA MN patch with initial concentration of 20% (w/v) was chosen. We next optimized the crosslinking time of GelMA MN patch. The mechanical test results indicated that longer crosslinking exposures led to stronger mechanical properties of GelMA MN patches (Figure 2F). However, the morphology of GelMA MN patches with ≥ 200 s crosslinking exposures maintained structural integrity while others were partially damaged by the degradation (Figure S4). Considering the time cost and swelling property, we chose crosslinking time of 200 s as the optimized condition.

Therefore, optimized GelMA MN patches were fabricated with a prepolymer concentration of 20% (w/v) and 200 s of crosslinking time. The swelling ratio at this condition was 324 ± 86% and the compressive modulus was 5.80 ± 1.41 MPa.

Fluid extraction and molecule detection (glucose and vancomycin) experiments were performed using agarose hydrogels and the results are presented in Figure 3. Figure 3A shows the process of fluid extraction and biomolecule detection using the GelMA MN patches. To simulate the fluid extraction, a GelMA MN patch was pressed against agarose hydrogels that contain specific concentrations of glucose and vancomycin. Then, the patch was removed and transferred to a centrifuge tube filled with DI water. After centrifugation, the analytes in the solution were tested. The appearance of GelMA MN patches after liquid extraction at different time points (0 min, 1 min, 10 min, 30 min and 24 h) are displayed in Figure 3B. The corresponding mass of liquid uptake at each time point is shown in Figure 3C. The GelMA MN patches showed equilibrated absorption of over 4 mg liquid per MN patch after swelling. Figure 3D displays the surface of the agarose hydrogel (2.0%, m/v) after treatment with the GelMA MN patch. Figure 3E and 3F show macroscopic images of the GelMA MN patches before and after extraction. Detected glucose concentrations were compared to the actual glucose concentrations in hydrogel and shown in Figure 3G. Glucose concentrations in the hydrogel were linearly varied from 50 to 600 mg/dL (shown in red). Detected glucose concentrations (shown in blue) were well-aligned with the actual concentration across the range of concentrations ($R^2 = 0.981$). In addition, a similar trend was also observed for vancomycin detection (Figure 3H). Vancomycin concentration in the hydrogel showed a good linearity from 1 to 16 μg/mL (blue dots). Detected concentrations were well-aligned with the pre-designed concentrations as $R^2 = 0.974$.

The results of ISF extraction and analysis *in vivo* are shown in Figure 4. The schematic (Figure 4A) describes the procedures used for ISF extraction and analysis, which is similar to the extraction of target molecules in agarose hydrogels. Wistar rats were utilized as a model and each rat was treated with GelMA MN patches on their dorsal side (Figure 4B). The magnified image of the treated skin is presented in Figure 4C. GelMA MNs efficiently penetrated the tissue as evidenced by the hematoxylin and eosin (H&E) staining (Figure S5). Figures 4D through 4H showed the recovery of the skin post-treatment. The MN punctures disappeared gradually as the skin recovered within 20 min of removing the patch. This indicates that minimal injury was caused and the procedure is, in fact, minimally invasive. The mass of ISF extracted at different treatment time points is shown in Figure 4I. ISF extraction gradually increased within 10 min of applying the MN patches and reached equilibrium after approximately 30 min. The mass of ISF collected in the GelMA MN patch was about 1.9 mg after 5 min and 2.5 mg after 10 min. Glucose and vancomycin were also utilized as model molecules for the *in vivo* test and the detected concentrations in ISF were compared to those in blood or plasma as shown in Figure 4J and 4K, respectively. The initial glucose concentrations of both samples were approximately 100 mg/dL for both in ISF and blood. Five minutes after intravenous glucose injection, glucose concentration in blood increased rapidly (179.6 ± 21.8 mg/dL) while only marginally increased in ISF (125.1 ± 28.3 mg/dL). However, glucose concentration reached a steady state 30 min after injection with a concentration of 170 mg/dL in both ISF and plasma. A similar trend was also observed for vancomycin detection. Five minutes after the injection, vancomycin concentration in plasma was 8.27 ± 0.13 μg/mL, while it displayed a smaller value (5.93 ± 0.18 μg/mL) in ISF. Over time the concentration of vancomycin in plasma and ISF reached

equilibrium: 30 min following injection, vancomycin concentrations in both fluids reached nearly 6.5 μg/mL and decreased to approximately 4 μg/mL 60 min after injection.

Agarose hydrogels are frequently used as models of skin as they can emulate the tissue to predict the *in vivo* performance of MNs, including ISF extraction[25] and drug release.[52] In our study, GelMA MN patches were used to extract glucose and vancomycin from agarose hydrogels. After applying the MN patch to the agarose, the shape and size of the patches changed significantly, indicating effective fluid extraction. Our results show that GelMA MNs can rapidly and efficiently extract both molecules from an agarose hydrogel. Our work demonstrates the utility of GelMA for diffusion-based ISF extraction which has been performed by other materials previously, such as polyvinyl alcohol, poly(methyl vinyl ether-alt-maleic acid) and poly(ethylene glycol).[53] The diffusion of ISF into polyvinyl alcohol-based MN patches has been studied and the results showed that only 0.30 μL of ISF could be collected by a single patch over the course of 12 h.[46] Biocompatible, hydrophilic materials have been created based on natural polymers and have been formed into MNs. Chang *et al.* demonstrated a methacrylated hyaluronic acid MN patch with the ability to withdraw about 2.3 μL of ISF within 10 min.[25] Compared to these studies, our GelMA MN patches also demonstrated sufficient ISF extraction capability *in vivo*. The GelMA patch collected about 2.5 mg of ISF (~ 2.5 μL) within 10 min. This improvement is the result of the excellent swelling properties of GelMA and the optimized prepolymer concentration and crosslinking time. While it may be possible to improve our design by incorporating designs such as hollow needles[54] or other features[14, 46, 53], the fabrication process of our current GelMA MN patch is simpler. These swellable patches are easy to manufacture and can collect ISF from the skin rapidly, making them promising for clinical applications. Moreover, skin recovers almost completely within 20 min of treatment, which further supports its use as a minimally-invasive transdermal ISF extraction device. The GelMA MN patch has advantages in lower fabrication cost and higher production yield comparing to HA-based MN patch, making it a competitive platform for translational studies. Furthermore, the nature-derived GelMA MN patch is derived from extracelluar matrix and possesses good biocompatibility as a medical device for sourcing ISF in a convenient and less invasive approach.

To compare the collection of ISF to blood, we also studied the detection of injected glucose and vancomycin molecules in skin-derived ISF compared to plasma. Both molecules were detectable and quantifiable in ISF, supporting existing research that ISF is a suitable fluid for diagnosis. Several studies about glucose or vancomycin detection also supported the concentration correlation between ISF and blood in the rat model.[14, 55] However, molecule concentrations in ISF displayed a hysteresis effect. Boyne *et al.* studied the dynamics of interstitial and blood glucose of patients with type I diabetes and observed a time lag of 4 min to 10 min in the change of interstitial glucose levels relative to blood glucose concentration.[56] The time lag of these metabolites or drugs may be caused by locations of metabolites and differing transport efficiencies between ISF and circulating blood. Since the target site of vancomycin, an antibiotic, is the local area surrounding an infected wound, the concentration of vancomycin in the local ISF provides more insight than that in blood. Kiang *et al.* have reviewed the pharmacokinetics of many antibiotics and reported a comprehensive summary on pharmacokinetic data suggested that some antibiotics, such as

vancomycin, are better suited for detection in ISF because their ISF concentration provides more information into the pharmacokinetic and pharmacodynamic relationships in the target region.[57] However, the pharmacokinetic characteristics of antibiotics in ISF are rarely reported which may be caused by the lack of facile and effective extraction approaches. Therefore, the GelMA MN patches that we have developed could serve as an effective tool in pharmacodynamic investigations.

In summary, a swellable GelMA MN patch for ISF extraction has been fabricated by using a micromolding method. The swelling and mechanical properties of the patch could be controlled by tuning the prepolymer concentration and crosslinking time. Lower concentrations of GelMA prepolymer lead to higher swelling ratios and lower compressive moduli. Glucose and vancomycin concentrations were comparable when detected in either ISF or plasma, demonstrating that the use of GelMA MN patches for ISF extraction from skin can be used to monitor the production and consumption of these molecules. Moreover, rapid recovery of the skin after removing the MN patches indicates that the patches exert minimally invasive fluid sampling. This technology has the potential to serve as a minimally invasive supplement or alternative to traditional blood sampling methods that are currently used in the clinic.

Experimental Section

GelMA preparation:

The GelMA prepolymer was prepared according to our previous work.[49] Briefly, 20 g of gelatin (type A from porcine skin, Sigma) was dissolved in 200 mL of DPBS under constant stirring at 60 °C. 16 mL of methacrylic anhydride was added gradually into the solution under vigorous stirring for 3 h at 50 °C. Afterwards, 1 L of DPBS (50 °C) was added. The residual methacrylic anhydride was removed by dialysis (12 −14 kDa membrane) at 50°C for 7 days. The GelMA prepolymer was obtained after lyophilization at −20 °C and was stored at 4 °C before use. The methacrylation to gelatin was assessed by proton nuclear magnetic resonance (^{1}H NMR) spectroscopy. The gelatin and GelMA were dissolved in D_2O at a concentration of 20 mg/mL, respectively. ^{1}H NMR spectra were obtained by Brucker AV400 broad band FT NMR spectrometer with 256 scans at room temperature. The degree of methacrylation, which was defined as the ratio of methacrylate groups to the total amino groups in gelatin prior to the reaction, were estimated from the integrated intensities according to the related works.[43–45]

GelMA MN preparation:

A specified amount of GelMA prepolymer (0.2 g, 0.3 g, 0.4 g, or 0.5 g) was dissolved in 2 mL of DI water at 50 °C and 10 mg of photoinitiator (Irgacure 2959, Sigma) was added at 60 °C. The GelMA solution was cast onto the PDMS mold and centrifuged for 5 min at 3500 rpm. The filled mold was exposed to 500 mW/cm^2 UV light (360 – 480 nm) for 10 s, 50 s, 100 s, 200 s, or 300 s. Following the exposure, the mold was kept away from light for 24h to dry the GelMA MNs. The GelMA MNs were subsequently peeled from the mold and stored at 4 °C before use.

Swelling of GelMA MN patches:

To calculate the swelling ratio of the GelMA MN patches, samples were incubated in DPBS for 1 min, 10 min, 30 min, and 24 h at 37 °C. After the specified durations, residual liquids on the surface of the patch were removed and the wet weights (W_w) were recorded. The dry weights (W_d) were measured after lyophilization and the swelling ratio was calculated as $[(W_w - W_d)/W_d] \times 100\%$. To predict the structural stability of swelled MNs *in vivo*, the GelMA MN patches with different crosslinking time (10 s, 50 s, 100 s, 200 s, and 300 s) were pressed against agarose hydrogel (2%, m/v) containing 2 U/mL of collagenase type II at 37 °C, respectively. 10 min later, the patches were peeled off and dried for scanning electron microscope (SEM) observation.

Mechanical properties of GelMA MN patches:

The mechanical properties of the patches were measured by a low-force mechanical testing system (5943 MicroTester, Instron, USA) according to the related work.[29, 42, 58] Briefly, The patch was placed needle-side up on a stainless-steel plate and compressed with a load cell at a rate of 1 mm/min up to the maximum loading force of 50 N. Correlations between the applied force and deformation of the patch were recorded during the whole testing process. The compressive modulus (E) represented the slope of stress (σ) - strain (ε) curve during the elastic deformation of the MNs and was calculated by $E = \sigma'/\varepsilon$. The stress (σ) and strain (ε) were calculated by $\sigma' = F/S$ and $\varepsilon = v(t - t_0)$, where F was the compressive force, S was the sectional area of the testing substance, v was the constant rate of the load cell (1 mm/min), t represented the time of elastic deformation, t_0 represented the time point when the load cell touch the top of testing substance (the force began to be recorded).

Skin penetration by GelMA MN patches:

The patches with different initial GelMA prepolymer concentration (15%, 20%, 25%) were pushed into the rat cadaver skin for 30 s, respectively. Trypan blue was used to stain the penetrated tissue after peeling off the patch. Excess trypan blue was washed by DPBS and the skin was imaged to check for the sign of penetrated *stratum corneum* (blue dots).

In vitro extraction and glucose and vancomycin detection:

Glucose and vancomycin were dissolved in 2% (m/v) agarose hydrogels to model ISF extraction *in vitro*. The concentrations of glucose were 50, 100, 200, 400, 600 mg/dL and the concentrations of vancomycin were 1, 2, 4, 8, 16 μg/mL. After the dry weight of the GelMA MN patch was recorded, the patch was pressed into the agarose hydrogel. Five minutes later, the MN patch was removed and the wet mass (W_w) of the patch was measured. The patch was then transferred into a centrifuge tube with 200 μL of DI water. After being centrifuged at 12000 rpm for 10 min, the solution in the tube was transferred for molecule quantification. The glucose concentration in the hydrogel was tested using a Glucose Assay Kit (Sigma) and the vancomycin concentration in hydrogel was tested using the LC-MS/MS system (API 4000) according to related work.[59] The mobile phase was distilled water – methanol (9:1, v/v) at a flow rate of 0.2 mL / min. The analytical column was a Gemini 5 μm NX-C18 (100 × 2 mm). Multiple reaction-monitoring (MRM) analyses were performed using transitions at m/z 725.5→144.0.

The detected concentration was calculated as $C = C_d \times V / [(W_w - W_d) \times \rho]$, in which C_d is the concentration of glucose detected by the kit or concentration of vancomycin detected by the LC-MS/MS system. V is the volume of DI water added into the centrifuge tube (200 μL), W_d is the dry weight of the GelMA MN patch, W_w is the wet weight of the GelMA MN patch after extraction, and ρ is the density of glucose or vancomycin solution (approximately 1.0 g/mL).

In vivo collection of ISF and glucose and vancomycin detection:

All animal experiments were approved by the Animal Care and Use Committee of University of California, Los Angeles, and procedures for animals were performed in accordance with the relevant guidelines and regulations. Wistar rats (4-week-old, approximately 70 – 80 g) were anesthetized with 50 mg/kg sodium pentobarbital. The dorsal hair of each rat was shaved. After the initial mass of the GelMA patch was weighed, it was applied to the dorsal skin of the rat using the thumb and index finger. Gauze was used to fix the patches on the skin. 10 min later, the patch was removed and the final mass was recorded. To quantify the concentration of the delivered molecules, the wet patch was transferred into a centrifuge tube with 200 μL of DI water. After centrifugation at 12000 rpm for 10 min, the solution in the tube was transferred to be tested. In addition, blood samples were also collected from the tail vein for glucose detection and the plasma was isolated *via* centrifugation for vancomycin detection. For histopathology, the skin was harvested and fixed in 10% neutral buffered formalin (BBC Biochemical, WA, USA), processed by a standard method, and embedded in paraffin. 4 μm in thickness tissue sections were stained with hematoxylin and eosin (H&E, BBC Biochemical) to confirm that GelMA MNs effectively penetrate the skin.

In the glucose detection experiment, the rats were intravenously injected with 1 mL of 0.2 g/mL glucose in saline. The glucose concentrations in ISF were tested using Glucose Assay Kit (Sigma) and the glucose levels in blood were tested using a glucometer (Clarity Diagnostics, US). In the vancomycin detection experiment, the rats were intravenously injected with 1 mL vancomycin at a concentration of 1 mg/mL in saline. The vancomycin concentration in ISF and plasma samples was also quantified by LC-MS/MS analysis (mentioned above).

Statistical analysis:

Analysis of variance (ANOVA) was used to test for statistical significance. The results were considered statistically significant when $P < 0.05$. All values are reported as mean ± standard deviation (S.D.).

Supplementary Material

Refer to Web version on PubMed Central for supplementary material.

Acknowledgements

The authors acknowledge funding from the National Institutes of Health (EB024403, EB023052, GM126831, and HL140618). J. Zhu also acknowledges the support from the Natural Science Foundation of Guangdong province, China (2018A0303130051).

References

[1]. Koka S, Beebe TJ, Merry SP, DeJesus RS, Berlanga LD, Weaver AL, Montori VM, Wong DT, J. Am. Dent. Assoc 2008, 139, 735. [PubMed: 18519997]

[2]. Kiang TK, Hafeli UO, Ensom MH, Clin. Pharmacokinet 2014, 53, 695. [PubMed: 24972859]

[3]. Raju KS, Taneja I, Singh SP, Wahajuddin, Biomed. Chromatogr 2013, 27, 1354. [PubMed: 23939915]

[4]. Nunes LA, Mussavira S, Bindhu OS, Biochem. Medica 2015, 25, 177.

[5]. Wiig H, Swartz MA, Physiol. Rev 2012, 92, 1005. [PubMed: 22811424]

[6]. Kool J, Reubsaet L, Wesseldijk F, Maravilha RT, Pinkse MW, D'Santos CS, van Hilten JJ, Zijlstra FJ, Heck AJ, Proteomics 2007, 7, 3638. [PubMed: 17890648]

[7]. Kiang TKL, Ranamukhaarachchi SA, Ensom MHH, Pharmaceutics 2017, 9, 43.

[8]. Muller AC, Breitwieser FP, Fischer H, Schuster C, Brandt O, Colinge J, Superti-Furga G, Stingl G, Elbe-Burger A, Bennett KL, J. Proteome. Res 2012, 11, 3715. [PubMed: 22578099]

[9]. Caffarel-Salvador E, Brady AJ, Eltayib E, Meng T, Alonso-Vicente A, Gonzalez-Vazquez P, Torrisi BM, Vicente-Perez EM, Mooney K, Jones DS, Bell SE, McCoy CP, McCarthy HO, McElnay JC, Donnelly RF, PloS one 2015, 10, e0145644. [PubMed: 26717198]

[10]. Sieg A, Guy RH, Delgado-Charro MB, Clin. Chem 2004, 50, 1383. [PubMed: 15155544]

[11]. Schmidt S, Banks R, Kumar V, Rand KH, Derendorf H, J. Clin. Pharmacol 2008, 48, 351. [PubMed: 18285620]

[12]. Voelkner NMF, Voelkner A, Costa J, Sy SKB, Hermes J, Weitzel J, Morales S, Derendorf H, Int. J. Antimicrob. Ag 2018, 51, 190.

[13]. Eltayib E, Brady AJ, Caffarel-Salvador E, Gonzalez-Vazquez P, Zaid Alkilani A, McCarthy HO, McElnay JC, Donnelly RF, Eur. J. Pharm Biopharm 2016, 102, 123 [PubMed: 26969262]

[14]. Kolluru C, Williams M, Yeh JS, Noel RK, Knaack J, Prausnitz MR, Biomed. Microdevices 2019, 21, 14. [PubMed: 30725230]

[15]. Xue P, Zhang L, Xu Z, Yan J, Gu Z, Kang Y, Appl. Mater. Today 2018, 13, 144.

[16]. Abdelghany S, Tekko IA, Vora L, Larraneta E, Permana AD, Donnelly RF, Pharmaceutics 2019, 11, 308.

[17]. Yu J, Zhang Y, Ye Y, DiSanto R, Sun W, Ranson D, Ligler FS, Buse JB, Gu Z, P. Natl. Acad. Sci. USA 2015, 112, 8260.

[18]. Wang J, Yu J, Zhang Y, Zhang X, Kahkoska AR, Chen G, Wang Z, Sun W, Cai L, Chen Z, Sci. Adv 2019, 5, eaaw4357. [PubMed: 31309150]

[19]. Joyce JC, Sella HE, Jost H, Mistilis MJ, Esser ES, Pradhan P, Toy R, Collins ML, Rota PA, Roy K, Skountzou I, Compans RW, Oberste MS, Weldon WC, Norman JJ, Prausnitz MR, J. Control. Release 2019, 304, 135. [PubMed: 31071375]

[20]. Zhu DD, Zhang XP, Yu HL, Liu RX, Shen CB, Zhang WF, Cui Y, Guo XD, Int. J. Pharmaceut 2019, 567, 118489.

[21]. Duong HTT, Kim NW, Thambi T, Giang Phan VH, Lee MS, Yin Y, Jeong JH, Lee DS, J. Control. Release 2018, 269, 225. [PubMed: 29154976]

[22]. Wang J, Wang Z, Yu J, Kahkoska AR, Buse JB, Gu Z, Adv. Mater 2019, 1902004

[23]. Paul R, Saville AC, Hansel JC, Ye Y, Ball C, Williams A, Chang X, Chen G, Gu Z, Ristaino JB, Wei Q, ACS nano 2019, 13, 6540. [PubMed: 31179687]

[24]. Mooney K, McElnay JC, Donnelly RF, Int. J. Pharm. Pract 2015, 23, 429. [PubMed: 25807981]

[25]. Chang H, Zheng M, Yu X, Than A, Seeni RZ, Kang R, Tian J, Khanh DP, Liu L, Chen P, Xu C, Adv. Mater 2017, 29, 1702243.

[26]. Zhang X, Chen G, Bian F, Cai L, Zhao Y, Adv. Mater 2019, e1902825. [PubMed: 31271485]

[27]. Al Sulaiman D, Chang JYH, Bennett NR, Topouzi H, Higgins CA, Irvine DJ, Ladame S, ACS nano 2019, 13, 9620. [PubMed: 31411871]

[28]. Paul R, Saville AC, Hansel JC, Ye Y, Ball C, Williams A, Chang X, Chen G, Gu Z, Ristaino JB, Wei Q, ACS nano 2019, 13, 6540. [PubMed: 31179687]

[29]. Luo Z, Sun W, Fang J, Lee K, Li S, Gu Z, Dokmeci MR, Khademhosseini A, Adv. Healthc. Mater 2019, 8, e1801054. [PubMed: 30565887]

[30]. O'Mahony C, Grygoryev K, Ciarlone A, Giannoni G, Kenthao A, Galvin P, J. Micromech. Microeng 2016, 26, 084005.

[31]. Gao J, Huang W, Chen Z, Yi C, Jiang L, Sens. Actuators B Chem 2019, 287, 102.

[32]. Lee D-S, Li CG, Ihm C, Jung H, Sens. Actuators B Chem 2018, 255, 384.

[33]. Pere CPP, Economidou SN, Lall G, Ziraud C, Boateng JS, Alexander BD, Lamprou DA, Douroumis D, Int. J. Pharm 2018, 544, 425. [PubMed: 29555437]

[34]. Das A, Singha C, Bhattacharyya A, Microelectron. Eng 2019, 210, 14.

[35]. Yan G, Warner KS, Zhang J, Sharma S, Gale BK, Int. J Pharm 2010, 391, 7. [PubMed: 20188808]

[36]. Bigi A, Cojazzi G, Panzavolta S, Roveri N, Rubini KJB, Biomaterials 2001, 22, 763. [PubMed: 11246944]

[37]. Bigi A, Cojazzi G, Panzavolta S, Roveri N, Rubini KJB, Biomaterials 2002, 23, 4827. [PubMed: 12361622]

[38]. Cao N, Fu Y, He J, Food Hydrocolloids 2007, 21, 575.

[39]. Li QY, Zhang JN, Chen BZ, Wang QL, Guo XD, RSC Advances 2017, 7, 15408.

[40]. Mandal A, Boopathy AV, Lam LK, Moynihan KD, Welch ME, Bennett NR, Turvey ME, Thai N, Van JH, Love JC, Sci. Transl. Med 2018, 10, eaar2227. [PubMed: 30429353]

[41]. Du H, Liu P, Zhu J, Lan J, Li Y, Zhang L, Zhu J, Tao J, ACS Appl Mater Interfaces 2019, 11, 43588. [PubMed: 31651148]

[42]. Lin S, Quan G, Hou A, Yang P, Peng T, Gu Y, Qin W, Liu R, Ma X, Pan X, Liu H, Wang L, Wu C, J Control Release 2019, 306, 69. [PubMed: 31145948]

[43]. Nichol JW, Koshy ST, Bae H, Hwang CM, Yamanlar S, Khademhosseini A, Biomaterials 2010, 31, 5536. [PubMed: 20417964]

[44]. Brinkman WT, Nagapudi K, Thomas BS, Chaikof ELJB, Biomacromolecules 2003, 4, 890. [PubMed: 12857069]

[45]. Ovsianikov A, Deiwick A, Van Vlierberghe S, Dubruel P, Moller L, Drager G, Chichkov B, Biomacromolecules 2011, 12, 851. [PubMed: 21366287]

[46]. Samant PP, Prausnitz MR, Proc. Natl. Acad. Sci. USA 2018, 115, 4583. [PubMed: 29666252]

[47]. Sun M, Sun X, Wang Z, Guo S, Yu G, Yang H, Polymers 2018, 10, 1290.

[48]. Zhao X, Lang Q, Yildirimer L, Lin ZY, Cui W, Annabi N, Ng KW, Dokmeci MR, Ghaemmaghami AM, Khademhosseini A, Adv. Healthc. Mater 2016, 5, 108. [PubMed: 25880725]

[49]. Loessner D, Meinert C, Kaemmerer E, Martine LC, Yue K, Levett PA, Klein TJ, Melchels FP, Khademhosseini A, Hutmacher DW, Nat Protoc 2016, 11, 727. [PubMed: 26985572]

[50]. Byambaa B, Annabi N, Yue K, Trujillo-de Santiago G, Alvarez MM, Jia W, Kazemzadeh-Narbat M, Shin SR, Tamayol A, Khademhosseini A, Adv. Healthc. Mater 2017, 6.

[51]. Zhu K, Shin SR, van Kempen T, Li YC, Ponraj V, Nasajpour A, Mandla S, Hu N, Liu X, Leijten J, Lin YD, Hussain MA, Zhang YS, Tamayol A, Khademhosseini A, Adv. Funct. Mater 2017, 27.

[52]. Than A, Liu C, Chang H, Duong PK, Cheung CMG, Xu C, Wang X, Chen P, Nat. Commun 2018, 9, 4433. [PubMed: 30401883]

[53]. Romanyuk AV, Zvezdin VN, Samant P, Grenader MI, Zemlyanova M, Prausnitz MR, Anal. Chem 2014, 86, 10520. [PubMed: 25367229]

[54]. Nicholas D, Logan KA, Sheng Y, Gao J, Farrell S, Dixon D, Callan B, McHale AP, Callan JF, Int. J. Pharm 2018, 547, 244. [PubMed: 29879505]

[55]. Moon BU, de Vries MG, Cordeiro CA, Westerink BH, Verpoorte E, Anal Chem 2013, 85, 10949. [PubMed: 24199633]

[56]. Boyne MS, Silver DM, Kaplan J, Saudek CD, Diabetes 2003, 52, 2790. [PubMed: 14578298]

[57]. Kiang TK, Schmitt V, Ensom MH, Chua B, Hafeli UO, J. Pharm. Sci 2012, 101, 4642. [PubMed: 22941939]

[58]. Raphael AP, Prow TW, Crichton ML, Chen X, Fernando GJ, Kendall MA, Small 2010, 6, 1785. [PubMed: 20665628]

[59]. Ito Y, Inagaki Y, Kobuchi S, Takada K, Sakaeda T, Int. J. Med. Sci 2016, 13, 271. [PubMed: 27076783]

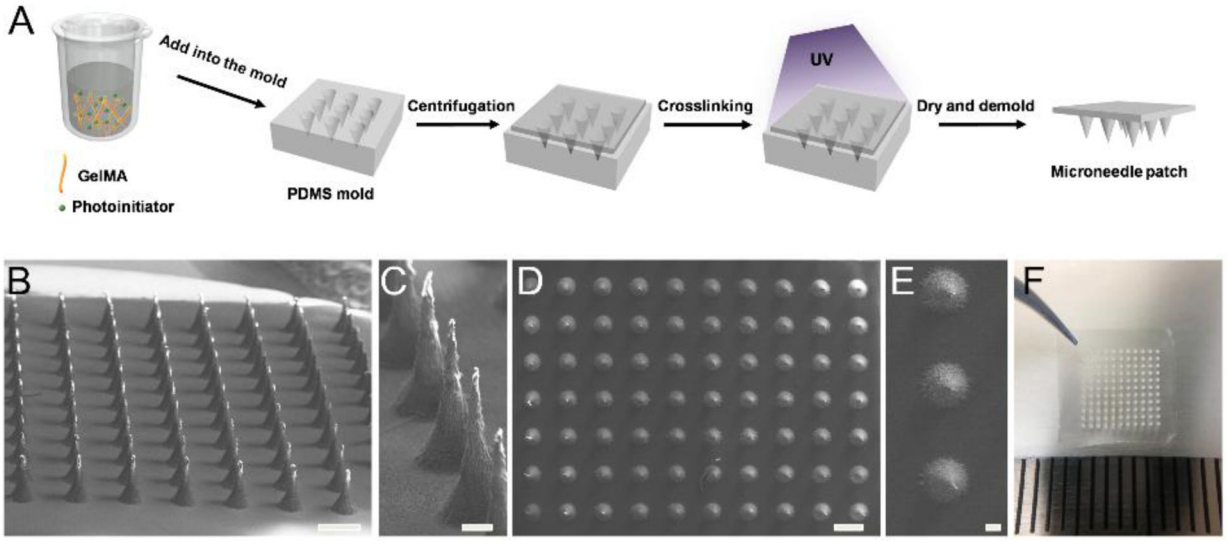

Figure 1.

Fabrication of the GelMA MN patch. (A) Schematic representation of the preparation process. Aqueous GelMA solution (aq) was cast into the PDMS mold. After centrifugation and UV crosslinking, the patch was dried and removed from the mold. (B, C) SEM images show the side view of GelMA MN array, (D, E) SEM images from the top view. Aligned conical needles were formed with an approximate height of 600 μm and bottom diameter of 300 μm. Scale bar : 500 μm in B, D and 100 μm in C, E. (F) A picture of the GelMA MN patch containing an 11 × 11 array of MNs over a 1 cm × 1 cm area.

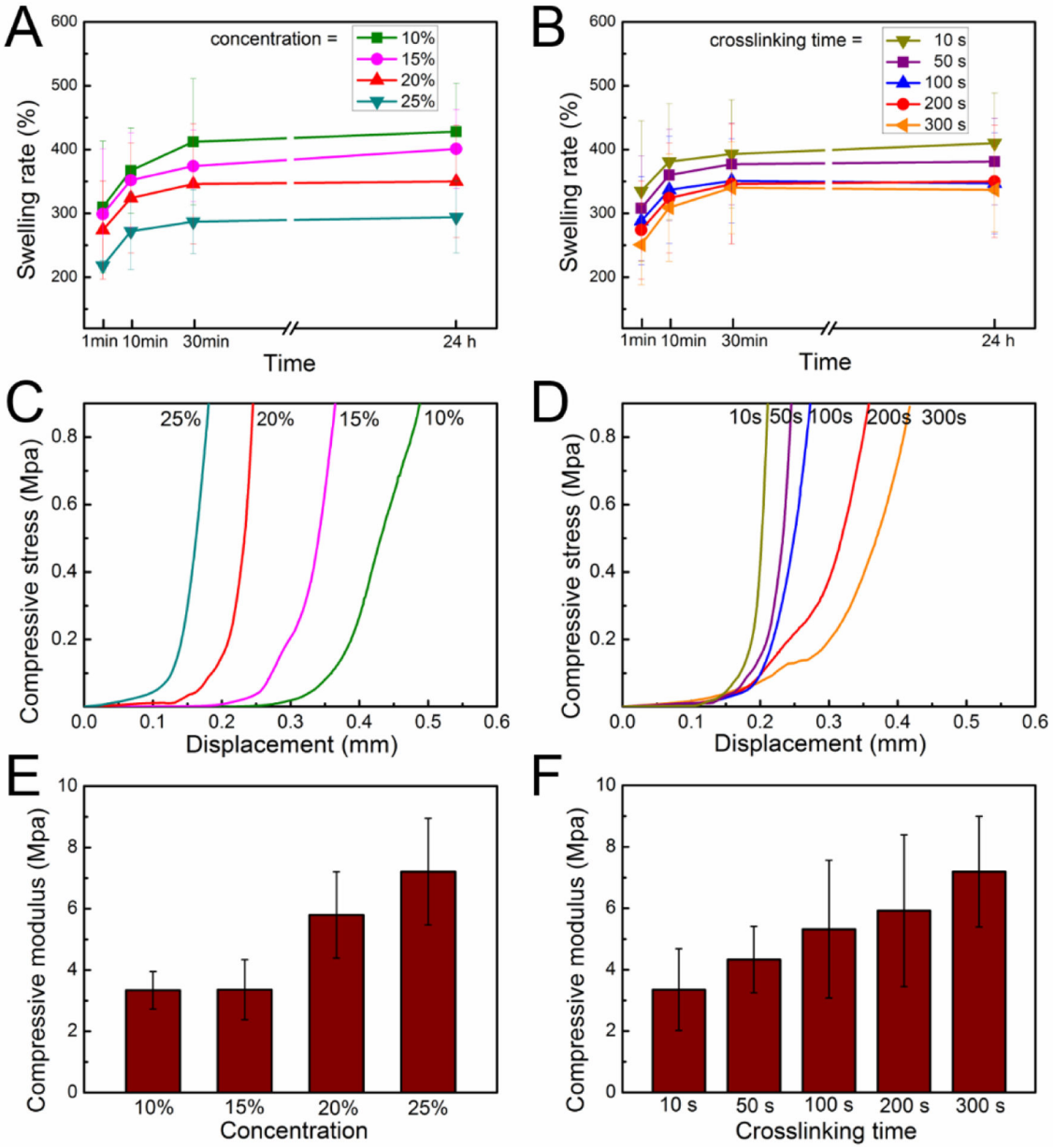

Figure 2.

Characterization of various GelMA MN patches. Swelling rate of the patches with different (A) GelMA concentrations (n = 5) and (B) crosslinking durations (n = 5). Stress-strain curve of patches with different (C) GelMA concentrations and (D) crosslinking durations. Compressive moduli of MNs with different (E) GelMA concentrations (n = 3) and (F) crosslinking durations (n = 3). The crosslinking time in (C) and (E) was set to 200 s. The initial GelMA concentration in (D) and (F) was 20% (m/v).

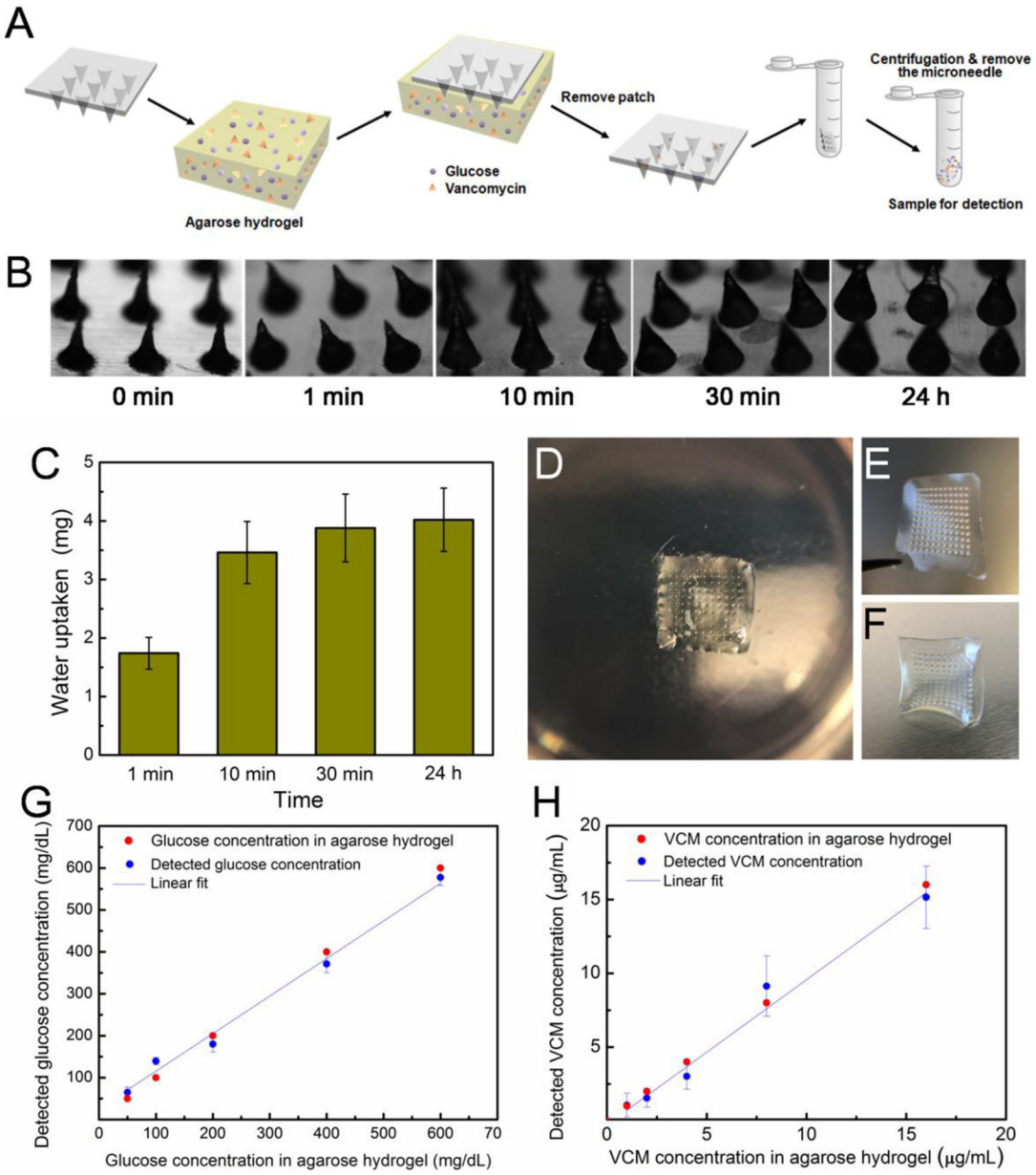

Figure 3.

Extraction process forthe detection of model molecules (glucose, vancomycin) *in vitro*. (A) Schematic representation of the extraction process. A GelMA MN patch was pressed against agarose hydrogel that was made with defined concentrations of glucose and vancomycin. Then, the patch was removed and transferred to a centrifuge with DI water. After centrifugation, the solution was tested. (B) Appearance of GelMA MN patch with different extraction durations (0 min, 1 min. 10 min, 30min, and 24 h). (C) Water uptake by hydrogel at different time points (n=5). (D) The GelMA MN patch was pressed against the hydrogel. Pictures of GelMA MN patch (E) before and (F) afterextraction. (G) Detected glucose concentration (blue dots) compared to the real glucose concentration (red dots) in hydrogel (n=3). The detected glucose concentration (blue dots) was fitted as a line (blue line), R^2 =

0.981. (H) Detected vancomycin (VCM) concentration (blue dots) compared to the real VCM concentration (red dots) in hydrogel (n=3). Detected VCM concentration (blue dots) was also fitted as a line (blue line), $R^2 = 0.974$.

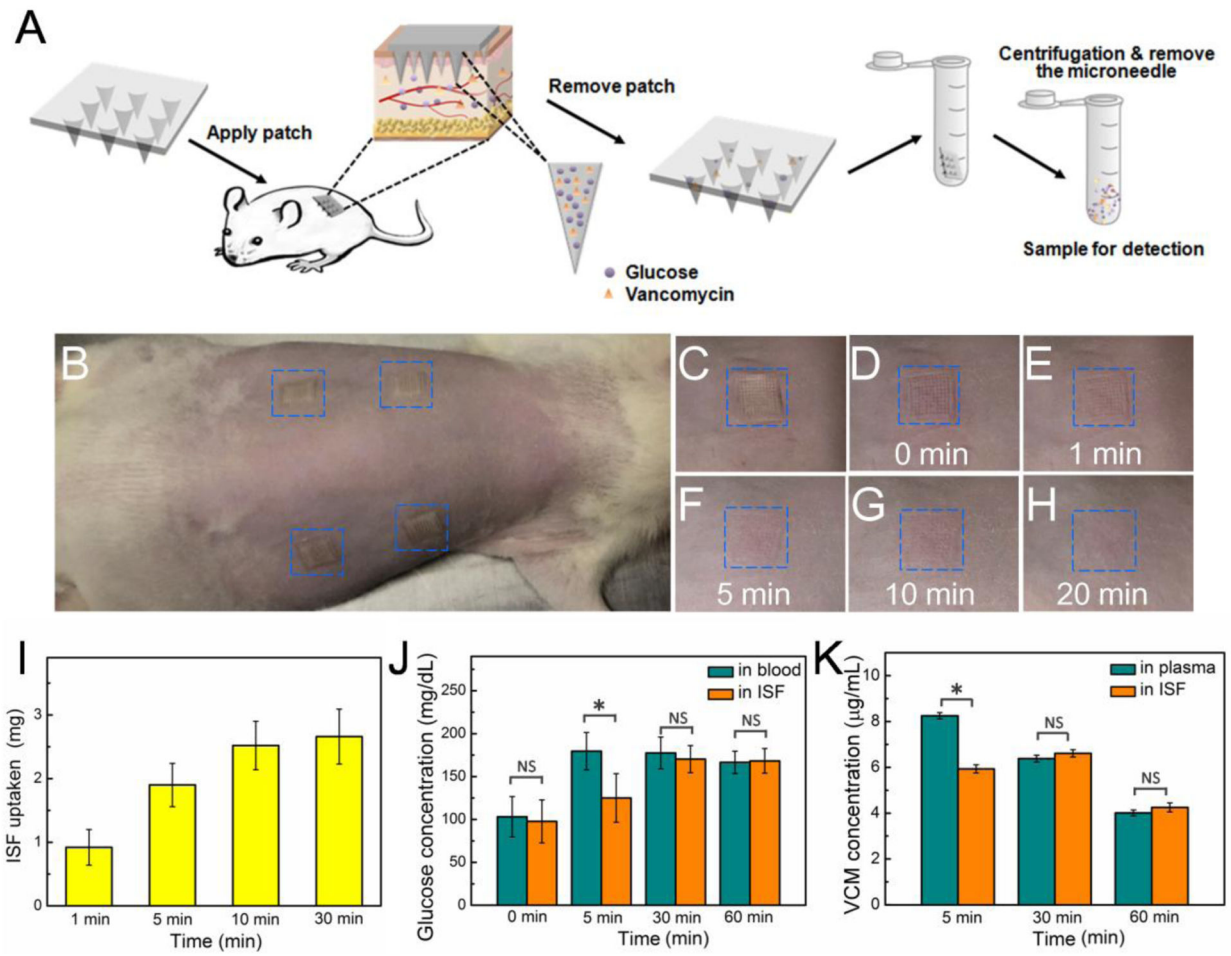

Figure 4.

ISF extraction process and detection of glucose and vancomycin (VCM) *in vivo*. (A) Schematic representation of the extraction process in a rat model. (B) Four GelMA MN patches were applied into the dorsal skin of a rat. (C) Magnified image of one patch on the skin. The skin recovery post treatment, (D) 0min, (E) 1min, (F) 5min, (G) 10min, (H), 20min. (I) Effect of ISF uptake at different timepoints (n=5). (J) Detected glucose concentrations in ISF compared to glucose concentrations in blood (n=5). (K) Detected VCM concentrations in ISF compared to VCM concentrations in plasma (n=5). *P< 0.05, NS means not significant.